


# *In-situ* deposited anti-aging TiN capping layer for Nb superconducting quantum circuits

Hao-Ran Tao(陶浩然), Lei Du(杜磊), Liang-Liang Guo(郭亮亮), Yong Chen(陈勇), Hai-Feng Zhang(张海峰), Xiao-Yan Yang(杨小燕), Guo-Liang Xu(徐国良), Chi Zhang(张 驰), Zhi-Long Jia(贾志龙), Peng Duan(段鹏), and Guo-Ping Guo(郭国平)

**Citation:**Chin. Phys. B, 2024, 33 (**9**): 090310. DOI: 10.1088/1674-1056/ad6a3c
Journal homepage: http://cpb.iphy.ac.cn; http://iopscience.iop.org/cpb

**What follows is a list of articles you may be interested in**

---

## Delayed-measurement one-way quantum computing on cloud quantum computer

Zhi-Peng Yang(杨智鹏), Yu-Ran Zhang(张煜然), Fu-Li Li(李福利), and Heng Fan(范桁)
Chin. Phys. B, 2024, 33 (**9**): 090304. DOI: 10.1088/1674-1056/ad6253

## A family of quantum von Neumann architecture

Dong-Sheng Wang(王东升)
Chin. Phys. B, 2024, 33 (**8**): 080302. DOI: 10.1088/1674-1056/ad50be

## Simulations of superconducting quantum gates by digital flux tuner for qubits

Xiao Geng(耿霄), Kaiyong He(何楷泳), Jianshe Liu(刘建设), and Wei Chen(陈炜)
Chin. Phys. B, 2024, 33 (**7**): 070305. DOI: 10.1088/1674-1056/ad47ab

## Electric field dependence of spin qubit in a Si-MOS quantum dot

Rong-Long Ma(马荣龙), Ming Ni(倪铭), Yu-Chen Zhou(周雨晨), Zhen-Zhen Kong(孔真真), Gui-Lei Wang(王桂磊), Di Liu(刘頔), Gang Luo(罗刚), Gang Cao(曹刚), Hai-Ou Li(李海欧), and Guo-Ping Guo(郭国平)
Chin. Phys. B, 2024, 33 (**6**): 060312. DOI: 10.1088/1674-1056/ad3812

## Fabrication of Al/AlO$_x$/Al Josephson junctions and superconducting quantum circuits by shadow evaporation and a dynamic oxidation process

Wu Yu-Lin (吴玉林), Deng Hui (邓辉), Yu Hai-Feng (于海峰), Xue Guang-Ming (薛光明), Tian Ye (田野), Li Jie (李洁), Chen Ying-Fei (陈莺飞), Zhao Shi-Ping (赵士平), Zheng Dong-Ning (郑东宁)
Chin. Phys. B, 2013, 22 (**6**): 060309. DOI: 10.1088/1674-1056/22/6/060309

---

**SPECIAL TOPIC — Quantum computing and quantum sensing**

# *In-situ* deposited anti-aging TiN capping layer for Nb superconducting quantum circuits

Hao-Ran Tao(陶浩然)[1,2], Lei Du(杜磊)[1,2], Liang-Liang Guo(郭亮亮)[1,2], Yong Chen(陈勇)[1,2], Hai-Feng Zhang(张海峰)[1,2], Xiao-Yan Yang(杨小燕)[1,2], Guo-Liang Xu(徐国良)[3], Chi Zhang(张驰)[3], Zhi-Long Jia(贾志龙)[3], Peng Duan(段鹏)[1,2,†], and Guo-Ping Guo(郭国平)[1,2,3,‡]

[1] *CAS Key Laboratory of Quantum Information, University of Science and Technology of China, Hefei* 230026, *China*
[2] *CAS Center for Excellence and Synergetic Innovation Center in Quantum Information and Quantum Physics, University of Science and Technology of China, Hefei* 230026, *China*
[3] *Origin Quantum Computing Company Limited, Hefei* 230088, *China*

(Received 18 June 2024; revised manuscript received 29 July 2024; accepted manuscript online 2 August 2024)

The performance of Nb superconducting quantum devices is predominantly limited by dielectric loss at the metal–air interface, where $Nb_2O_5$ is considered the main loss source. Here, we suppress the formation of native oxides by *in-situ* deposition of a TiN capping layer on the Nb film. With TiN capping layers, no $Nb_2O_5$ forms on the surface of the Nb film. The quality factor $Q_i$ of the Nb resonator increases from $5.6 \times 10^5$ to $7.9 \times 10^5$ at low input power and from $6.8 \times 10^6$ to $1.1 \times 10^7$ at high input power. Furthermore, the TiN capping layer also shows good aging resistance in Nb resonator devices, with no significant performance fluctuations after one month of aging. These findings highlight the effectiveness of TiN capping layers in enhancing the performance and longevity of Nb superconducting quantum devices.

**Keywords:** anti-aging, oxidation, dielectric loss, Nb superconducting quantum circuits

**PACS:** 03.67.Lx, 03.67.–a **DOI:** 10.1088/1674-1056/ad6a3c

## 1. Introduction

Dielectric loss at material interfaces significantly impacts the coherence time of qubits and the quality factors of superconducting resonators.[1–5] In superconducting quantum devices, lossy dielectrics associated with two-level systems (TLSs) are present at metal–air (MA), metal–substrate (MS), and substrate–air (SA) interfaces.[6–8] Advances in geometric design,[9–12] material selection,[13,14] and fabrication processes[15–17] have led to substantial reductions in the dielectric loss over the past decade. However, native oxide-related loss in superconducting quantum devices remains a persistent issue, especially when samples are exposed to air for extended periods. The issue of aging arises with the gradual degradation of device performance due to the formation and growth of native oxides over time.

Superconducting quantum chips are susceptible to degradation over time when exposed to ambient conditions. The aging is a critical issue that can significantly impact the performance and reliability of quantum computing devices. The aging often occurs through chemical reactions, such as oxidation of superconducting films in air, leading to an increase in the dielectric loss. The anti-aging properties of superconducting quantum chips are vital for maintaining high performance, ensuring long-term stability, and enabling scalability of quantum computations. Understanding the mechanisms of aging and developing strategies to mitigate its effects are essential for the continued advancement and practical deployment of quantum technologies.

Nb is widely utilized in the fabrication of superconducting quantum devices[18–20] due to its favorable physical properties[21] and compatibility with post-treatment processes.[22] Nb is also utilized in the fabrication of high-quality superconductor–semiconductor heterojunctions[23] and hybrid superconducting tunnel junctions.[24] However, Nb suffers from significant aging issues. When exposed to air, a native oxide layer approximately 5 nm thick, consisting of NbO, $NbO_2$, and $Nb_2O_5$, forms instantaneously on its surface.[25–27] Among these, $Nb_2O_5$ is the primary factor responsible for degrading the coherence time of qubits and the quality factors of superconducting resonators. According to the interface participation ratio model,[8,28] a thicker $Nb_2O_5$ layer leads to a larger MA participation ratio, thereby increasing the dielectric loss. Therefore, suppressing TLS losses by removing or preventing the formation of $Nb_2O_5$ is crucial for the implementation of high-performance superconducting quantum devices.

To date, various solutions have been developed to remove the native oxide on the surface of Nb films. Wet etching in HF effectively eliminates the native oxide in a short time.[22] Additionally, heat treatment above 350 °C in a vacuum leads to the decomposition of $Nb_2O_5$ into NbO or $NbO_2$.[29,30] How-

†Corresponding author. E-mail: pengduan@ustc.edu.cn
‡Corresponding author. E-mail: gpguo@ustc.edu.cn

© 2024 Chinese Physical Society and IOP Publishing Ltd 

ever, the regrowth of native oxides is inevitable upon air exposure. These post-treatment schemes show poor aging resistance. Moreover, these post-treatment processes are often incompatible with the intricate fabrication processes of superconducting quantum devices. Implementing superconducting capping layers has proven effective in addressing the issue of secondary oxidation.[29,31] Capping layers such as Al, Au, TiN, and Ta can be fabricated on the base Nb films to prevent oxidation. Among these, the TiN capping layer is the best candidate for compatibility with large-scale superconducting qubit devices because TiN serves as an under-bump metallization (UBM) layer necessary for flip-chip design.[32] To achieve high-quality TiN capping layers, the *in-situ* deposition of Nb and TiN in the same vacuum chamber is particularly significant, as the transfer deposition scheme with vacuum break inevitably results in surface oxidation of Nb, given the rapid nature of this process. Understanding the anti-aging properties of the capping layers is essential for enhancing the longevity and scalability of superconducting quantum circuits.

In this study, we utilized *in-situ* deposition to fabricate an 80 nm Nb film and a 10 nm TiN capping layer without breaking the vacuum. Characterization of the interface between the Nb film and the TiN capping layer revealed that the *in-situ* deposited TiN capping layer effectively suppressed the formation of $Nb_2O_5$. As a result, the performance of TiN-capped Nb superconducting resonators improved significantly. To assess the anti-aging properties of the TiN capping layer, we measured the quality factors ($Q_i$) of Nb resonators and TiN-capped Nb resonators both before and after one month of aging. The results showed a significant decrease in the $Q_i$ of the Nb resonators post-aging, whereas the $Q_i$ of the TiN-capped Nb resonators remained unchanged, demonstrating the superior aging resistance of the TiN capping layer. The XPS characterization results indicated that even after one month of aging, the TiN layer effectively prevented the formation of $Nb_2O_5$ on the Nb film.

## 2. Fabrication and method

We characterized the performance of the TiN capping layers through measurements of resonators. Nb resonators were fabricated on high resistivity ($>$ 10 kΩ·cm) intrinsic (100) plane silicon substrates. The substrates were initially rinsed with buffered oxide etch (BOE) to remove surface oxides. Subsequently, the wafers were immediately loaded into a high vacuum sputter chamber to deposit an 80 nm Nb film. For the TiN-capped Nb resonators, a 10 nm TiN film was deposited *in-situ* without breaking the vacuum to prevent the formation of an oxide layer between the Nb and TiN films. After the deposition of the superconducting films, a positive photoresist SPR955 was spun onto the wafers, and standard photolithography techniques were employed to define the resonator pattern. The patterned films were etched using $CF_4$ plasma in a reactive ion etching (RIE) system. The photoresist mask was removed from the wafers using an NMP bath at 80 °C. To further eliminate residues introduced during the fabrication processes, the wafers were immersed in diluted hydrofluoric acid (HF) for 20 s and subsequently rinsed with deionized water.

The performance of a resonator is intricately tied to both its geometric design and fabrication process. To facilitate a rigorous comparison, we ensured uniformity in the structure of the two sample types: Nb resonators and TiN-capped Nb resonators. Figure 1 presents a scanning electron microscope (SEM) image of the resonator. Each chip contains 12 superconducting coplanar waveguide (CPW) quarter-wave resonators with a center trace width ($w$) of 10 μm and gap ($g$) of 5 μm, all of which are capacitively coupled to the transmission line, with resonance frequencies ranging from 6 GHz to 7 GHz. The consistency of the planar two-dimensional (2D) structure was meticulously maintained through careful layout design. According to the loss participation ratio model, the dielectric loss of the resonator is intricately linked to the morphology of the channel etching.[8] Hence, we conducted an exhaustive series of tests on various etching recipes to ensure that the etching channel morphology, depth, and roughness of the two samples remain similar. Table 1 summarizes the geometric characterization results of the two samples, indicating an etching depth of approximately 170 nm and a roughness ($R_q$) of approximately 1 nm for SA and MA interfaces. By upholding uniformity in the geometry and fabrication process of the two samples, the participation ratios of both types are practically consistent. Consequently, any discrepancy in dielectric loss is primarily attributed to the dielectrics at the MA interface.

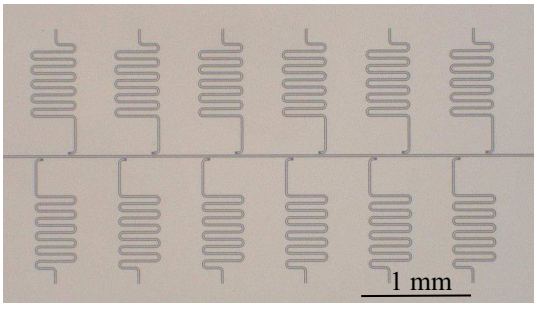



**Fig. 1.** SEM image of the resonator. Each chip contains 12 CPW quarter-wave resonators, all of which are capacitively coupled to the transmission line.

**Table 1.** Comparison of geometric parameters between the Nb resonator and TiN-capped Nb resonator

| Sample | Geometric parameters | | |
|---|---|---|---|
| | Depth | $R_{q1}$[a] | $R_{q2}$[b] |
| Nb resonator | 172 nm | 1.06 nm | 0.88 nm |
| TiN-capped Nb resonator | 170 nm | 1.11 nm | 0.89 nm |

[a]It represents the roughness of SA interface.
[b]It represents the roughness of MA interface.

## 3. Characterization and analysis

The resonators were measured inside a dilution refrigerator at a temperature of approximately 20 mK. The resonators were measured using a vector network analyzer (VNA) to obtain the transmission scattering parameter $S_{21}$ of the transmission line. The $Q_i$ of the resonator was then extracted through circle fitting at different input microwave powers.[33,34] At low photon numbers, $Q_i$ is dominated by TLSs, which becomes saturated at higher photon numbers. Figure 2 shows the dependence of $Q_i$ on the number of photons for the two types of samples. The Nb resonator exhibited a $Q_i$ of approximately $5.6 \times 10^5$ at low input microwave power, while the TiN-capped Nb resonators demonstrated a significantly higher $Q_i$ of $7.9 \times 10^5$. At high input power, the $Q_i$ of the TiN-capped Nb resonator was $1.1 \times 10^7$, compared to $6.8 \times 10^6$ for the Nb resonator. Figures 2(a) and 2(b) illustrate the statistical results of $Q_i$ for both samples at low and high input powers. These results clearly indicate that the TiN capping layer markedly improves the performance of superconducting Nb quantum devices.

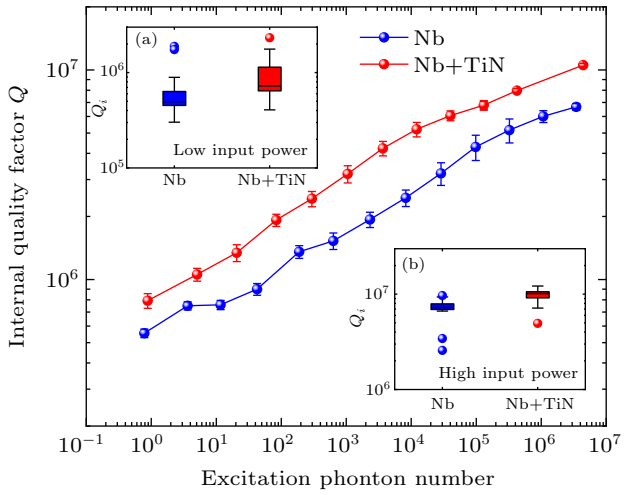



**Fig. 2.** The quality factor $Q_i$ of resonators vs. the average photon population $\langle n_p \rangle$. Blue curve represents Nb resonators and red curve represents TiN-capped Nb resonators. Insets: (a) the statistical results of $Q_i$ at single photon regime ($\langle n_p \rangle \sim 1$), (b) the statistical results of $Q_i$ at high photon regime ($\langle n_p \rangle > 3 \times 10^6$). Each boxplot represents the median (black line within the box), 25% to 75% values (whiskers), interquartile range (box boundaries), extreme value (error bar) and outliers (red and blue circles).

To further examine the anti-aging property of the TiN capping layer on Nb resonators, we exposed both Nb and TiN-capped Nb resonators to ambient air for natural aging over the course of one month. After this aging period, the samples were returned to the low-temperature environment for remeasurement. As shown in Fig. 3, the Nb resonators experienced a significant decrease in $Q_i$, dropping from $6.0 \times 10^5$ to $3.7 \times 10^5$ at low input power and from $7.1 \times 10^6$ to $5.9 \times 10^6$ at high input power. In contrast, the $Q_i$ of the TiN-capped Nb resonators remained stable, showing no significant decline. These results demonstrate that the TiN capping layer effectively protects Nb resonators from degradation due to aging.

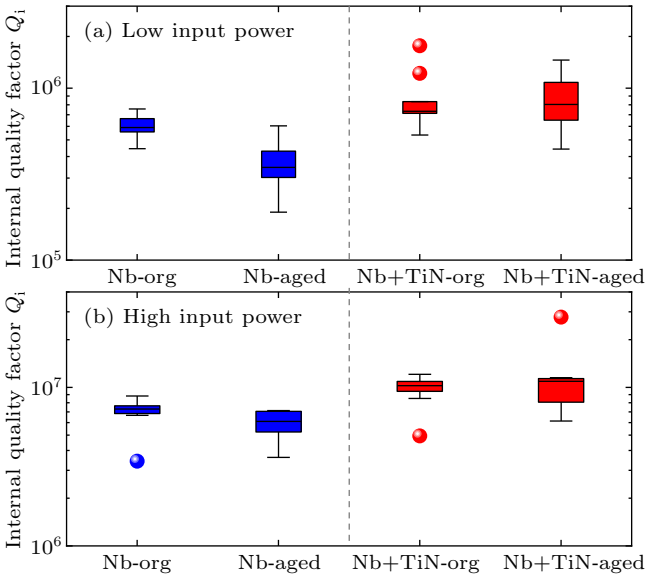



**Fig. 3.** (a) The $Q_i$ of resonators before and after aging at low input power. (b) The $Q_i$ of resonators before and after aging at high input power. The suffixes "org" and "aged" denote samples taken before and after the aging process, respectively.

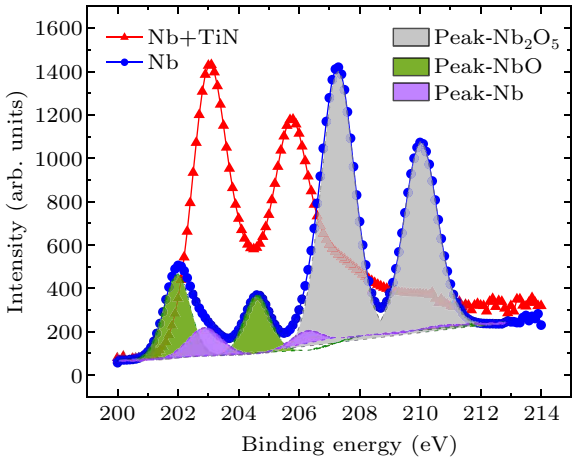



**Fig. 4.** The XPS spectra of the surface of the Nb film and the interface between Nb and TiN films. Spectroscopic peaks corresponding to $Nb_2O_5$, NbO and Nb are shown individually through peak fitting.

The superiority and anti-aging performance of the TiN capping layer on the Nb film are primarily due to its ability to prevent the formation of oxide layers. The complex native oxide that forms on the surface of Nb films comprises NbO, $NbO_2$, and $Nb_2O_5$, with $Nb_2O_5$ being the primary source of microwave loss. Previous research has indicated that microwave loss scales linearly with the thickness of $Nb_2O_5$, and the thickness of $Nb_2O_5$ increases linearly with exposure time to ambient air.[35] We used x-ray photoelectron spectroscopy (XPS) to characterize the surface atomic species of these samples. The XPS system employed *in-situ* Ar ion milling to facilitate analysis at various depths. Figure 4 presents the XPS spectra of the surface of Nb film and the interface between Nb and TiN films. The result indicates the presence of $Nb_2O_5$ and

NbO on the Nb film surface, with a significantly high spectral peak corresponding to $Nb_2O_5$. Conversely, the interface between Nb and TiN films is predominantly characterized by Nb peaks. These findings preliminarily demonstrate that the TiN capping layer effectively suppresses the formation of oxides on the Nb film surface. It is undeniable that a certain oxide layer $TiO_x$ will also form on the surface of TiN film, but $Nb_2O_5$ remains the dominant source of loss for the TiN-capped Nb samples.[31]

We further analyzed the native oxide composition at different depths of the films from the XPS spectra. As illustrated in Figs. 5(a) and 5(c), the surface of the Nb film exhibits a complex native oxide layer approximately 2 nm thick, with $Nb_2O_5$ confined to the top 1 nm. In contrast, at the interface between the TiN capping layer and the Nb film, no $Nb_2O_5$ is detected; only a tiny amount of NbO is present. The NbO extends nearly across the entire surface of the bulk Nb, likely due to the diffusion of oxygen molecules.[26] It demonstrates that *in-situ* deposition within the same chamber effectively prevents the formation of the lossy $Nb_2O_5$ on the surface of Nb film. Combining measurement results above, it is easy to draw a conclusion that removing the native $Nb_2O_5$ on the surface of Nb film improves the performance of Nb superconducting quantum devices.

Figures 5(b) and 5(d) show the native oxide composition results of the aged samples. After one month of aging in ambient air, the thickness of the native oxides on the Nb film increased to approximately 5 nm, with the $Nb_2O_5$ layer reaching 2 nm. For the TiN-capped Nb film, the content of NbO at the interface showed almost no change, and no other oxides were formed. Moreover, $Nb_2O_5$ was not detected throughout the entire TiN-capped film. It indicates that TiN exhibits excellent anti-aging properties on the Nb film, effectively preventing the oxidation of the Nb film. Enhanced anti-aging properties contribute to a longer operational lifespan and easier scalability for quantum devices.

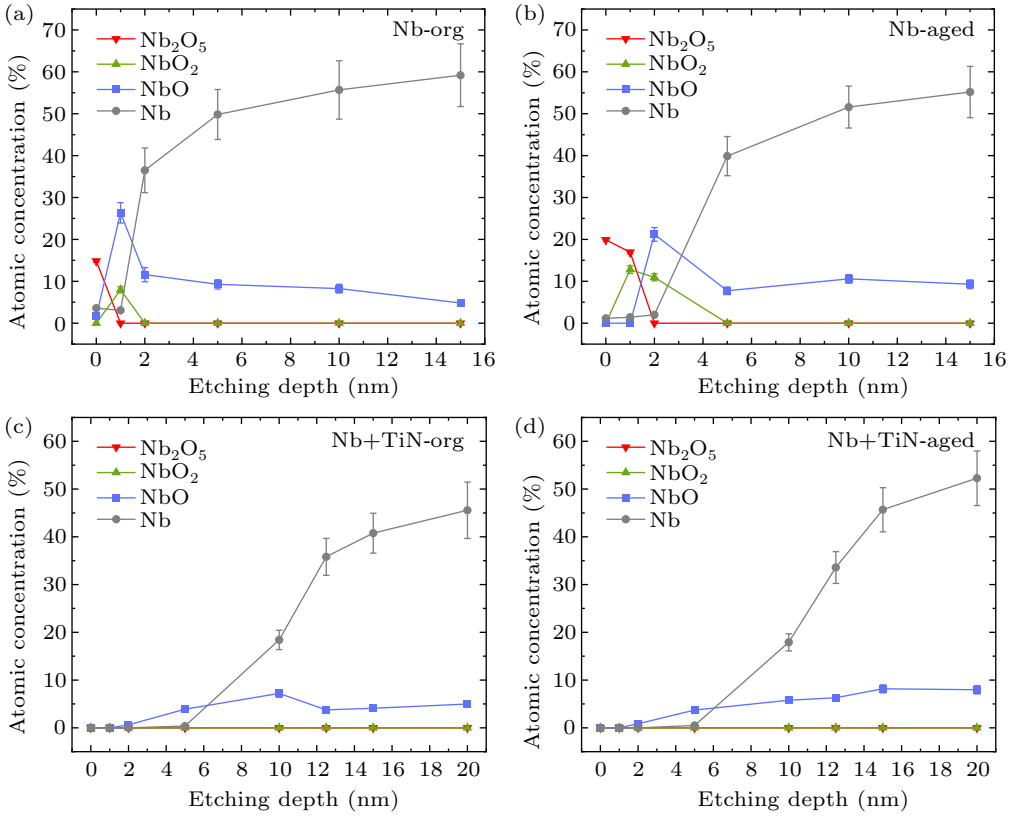



**Fig. 5.** The native oxide composition results for various depths of Nb films and TiN-capped Nb films. (a) and (b) correspond respectively to the Nb films before and after aging. (c) and (d) correspond respectively to the TiN-capped Nb films before and after aging. The curves of different colors illustrate the variations in the trends of various oxide contents.

## 4. Conclusion

In conclusion, our study demonstrates the efficacy of *in-situ* deposition of a 10 nm TiN capping layer on Nb films in suppressing the formation of lossy $Nb_2O_5$, thereby optimizing the performance of Nb-based superconducting quantum devices. Specifically, we observed a notable enhancement in the $Q_i$ of Nb resonators at both low and high input powers. Moreover, our investigation underscores the excellent aging resistance of the TiN capping layer in Nb resonator devices, as evidenced by the absence of significant performance fluctuations even after one month of aging. These findings highlight the promising potential of TiN capping layers for advancing the development of high-performance, long-term stable, and scalable superconducting quantum devices.

## Acknowledgments

Project supported by the National Natural Science Foundation of China (Grant Nos. 12034018 and 11625419). This work was partially carried out at the USTC Center for Micro and Nanoscale Research and Fabrication.

## References

[1] Murray C E 2021 *Mater. Sci. Eng. R Reports* **146** 100646
[2] Pappas D P, Vissers M R, Wisbey D S, Kline J S and Gao J 2011 *IEEE Trans. Appl. Supercond.* **21** 871
[3] Sage J M, Bolkhovsky V, Oliver W D, Turek B and Welander P B 2011 *J. Appl. Phys.* **109** 063915
[4] Martinis J M, Cooper K B, McDermott R, Steffen M, Ansmann M, Osborn K D, Cicak K, Oh S, Pappas D P, Simmonds R W and Yu C C 2005 *Phys. Rev. Lett.* **95** 210503
[5] Lisenfeld J, Bilmes A, Megrant A, Barends R, Kelly J, Klimov P, Weiss G, Martinis J M and Ustinov A V 2019 *npj Quantum Inf.* **5** 105
[6] Sandberg M, Vissers M R, Kline J S, Weides M, Gao J, Wisbey D S and Pappas D P 2012 *Appl. Phys. Lett.* **100** 262605
[7] Calusine G, Melville A, Woods W, Das R, Stull C, Bolkhovsky V, Braje D, Hover D, Kim D K, Miloshi X, Rosenberg D, Sevi A, Yoder J L, Dauler E and Oliver W D 2018 *Appl. Phys. Lett.* **112** 262605
[8] Wenner J, Barends R, Bialczak R C, Chen Y, Kelly J, Lucero E, Mariantoni M, Megrant A, O'Malley P J J, Sank D, Vainsencher A, Wang H, White T C, Yin Y, Zhao J, Cleland A N and Martinis J M 2011 *Appl. Phys. Lett.* **99** 1
[9] Lahtinen V and Möttönen M 2020 *J. Phys. Condens. Matter* **32** 405702
[10] Geerlings K, Shankar S, Edwards E, Frunzio L, Schoelkopf R J and Devoret M H 2012 *Appl. Phys. Lett.* **100** 1
[11] He H, Wang W, Liu F, Yuan B and Shan Z 2022 *Entropy* **24** 952
[12] Eun S, Park S H, Seo K, Choi K and Hahn S 2023 *J. Phys. D: Appl. Phys.* **56** 505306
[13] Deng H, Song Z, Gao R, Xia T, Bao F, Jiang X, Ku H S, Li Z, Ma X, Qin J, Sun H, Tang C, Wang T, Wu F, Yu W, Zhang G, Zhang X, Zhou J, Zhu X, Shi Y, Zhao H H and Deng C 2023 *Phys. Rev. Appl.* **19** 024013
[14] Lock E H, Xu P, Kohler T, Camacho L, Prestigiacomo J, Rosen Y J and Osborn K D 2019 *IEEE Trans. Appl. Supercond.* **29** 1
[15] Mergenthaler M, Müller C, Ganzhorn M, Paredes S, Müller P, Salis G, Adiga V P, Brink M, Sandberg M, Hertzberg J B, Filipp S and Fuhrer A 2021 *npj Quantum Inf.* **7** 157
[16] Wang C, Li X, Xu H, Li Z, Wang J, Yang Z, Mi Z, Liang X, Su T, Yang C, Wang G, Wang W, Li Y, Chen M, Li C, Linghu K, Han J, Zhang Y, Feng Y, Song Y, Ma T, Zhang J, Wang R, Zhao P, Liu W, Xue G, Jin Y and Yu H 2022 *npj Quantum Inf.* **8** 3
[17] Zikiy E V, Ivanov A I, Smirnov N S, Moskalev D O, Polozov V I, Matanin A R, Malevannaya E I, Echeistov V V, Konstantinova T G and Rodionov I A 2023 *Sci. Rep.* **13** 15536
[18] Kwon S, Fadavi Roudsari A, Benningshof O W B, Tang Y C, Mohebbi H R, Taminiau I A J, Langenberg D, Lee S, Nichols G, Cory D G and Miao G X 2018 *J. Appl. Phys.* **124** 033903
[19] Dominjon A, Shu S, Kroug M, Noguchi T, Sekimoto Y, Shan W, Sekiguchi S and Nitta T 2019 *J. Low Temp. Phys.* **194** 404
[20] Bruno A, Mengucci P, Mercaldo L V and Lisitskiy M P 2013 *Supercond. Sci. Technol.* **26** 035004
[21] Annunziata A J, Santavicca D F, Frunzio L, Catelani G, Rooks M J, Frydman A and Prober D E 2010 *Nanotechnology* **21** 445202
[22] Altoé M V P, Banerjee A, Berk C, Hajr A, Schwartzberg A, Song C, Ghadeer M A, Aloni S, Elowson M J, Kreikebaum J M, Wong E K, Griffin S, Rao S, Weber-Bargioni A, Minor A M, Santiago D I, Cabrini S, Siddiqi I and Ogletree D F 2020 arXiv:2012.07604
[23] Hu Z W and Qiu X G 2023 *Chin. Phys. B* **32** 037401
[24] Liu B L, Liu D, Yao M, Jin J D, Wang Z, Li J, Shi S C, Chekushkin A, Fominsky M, Filippenko L and Koshelets V 2024 *Chin. Phys. B* **33** 058501
[25] Sebastian J, Seidman D, Yoon K, Bauer P, Reid T, Boffo C and Norem J 2006 *Physica C* **441** 70
[26] Delheusy M, Stierle A, Kasper N, Kurta R P, Vlad A, Dosch H, Antoine C, Resta A, Lundgren E and Andersen J 2008 *Appl. Phys. Lett.* **92** 101911
[27] Romanenko A and Schuster D I 2017 *Phys. Rev. Lett.* **119** 264801
[28] Wang C, Axline C, Gao Y Y, Brecht T, Chu Y, Frunzio L, Devoret M H and Schoelkopf R J 2015 *Appl. Phys. Lett.* **107** 162601
[29] Proslier T, Zasadzinski J, Moore J, Pellin M, Elam J, Cooley L, Antoine C, Norem J and Gray K E 2008 *Appl. Phys. Lett.* **93** 10
[30] Semione G D L, Pandey A D, Tober S, Pfrommer J, Poulain A, Drnec J, Schütz G, Keller T F, Noei H, Vonk V, Foster B and Stierle A 2019 *Phys. Rev. Accel. Beams* **22** 103102
[31] Bal M, Murthy A A, Zhu S, Crisa F, You X, Huang Z, Roy T, Lee J, van Zanten D, Pilipenko R, Nekrashevich I, Lunin A, Bafia D, Krasnikova Y, Kopas C J, Lachman E O, Miller D, Mutus J Y, Reagor M J, Cansizoglu H, Marshall J, Pappas D P, Vu K, Yadavalli K, Oh J S, Zhou L, Kramer M J, Lecocq F, Goronzy D P, Torres-Castanedo C G, Pritchard P G, Dravid V P, Rondinelli J M, Bedzyk M J, Hersam M C, Zasadzinski J, Koch J, Sauls J A, Romanenko A and Grassellino A 2024 *npj Quantum Inf.* **10** 43
[32] Foxen B, Mutus J Y, Lucero E, Graff R, Megrant A, Chen Y, Quintana C, Burkett B, Kelly J, Jeffrey E, Yang Y, Yu A, Arya K, Barends R, Chen Z, Chiaro B, Dunsworth A, Fowler A, Gidney C, Giustina M, Huang T, Klimov P, Neeley M, Neill C, Roushan P, Sank D, Vainsencher A, Wenner J, White T C and Martinis J M 2018 *Quantum Sci. Technol.* **3** 014005
[33] Megrant A, Neill C, Barends R, Chiaro B, Chen Y, Feigl L, Kelly J, Lucero E, Mariantoni M, O'Malley P J J, Sank D, Vainsencher A, Wenner J, White T C, Yin Y, Zhao J, Palmstrøm C J, Martinis J M and Cleland A N 2012 *Appl. Phys. Lett.* **100** 113510
[34] Probst S, Song F B, Bushev P A, Ustinov A V and Weides M 2015 *Rev. Sci. Instrum.* **86** 024706
[35] Verjauw J, Potočnik A, Mongillo M, Acharya R, Mohiyaddin F, Simion G, Pacco A, Ivanov T, Wan D, Vanleenhove A, Souriau L, Jussot J, Thiam A, Swerts J, Piao X, Couet S, Heyns M, Govoreanu B and Radu I 2021 *Phys. Rev. Appl.* **16** 014018